Advances in Nano Research, *Vol. 13, No.5 (2022) 437-451*
https://doi.org/10.12989/anr.2022.13.5.437

Synthesis and spectroscopic characterization of zinc ferrite nanoparticles

Shefali Arora[1], Subhajit Nandy[2], Mamta Latwal*[1], Ganesh Pandey[3], Jitendra P. Singh[4] and Keun H. Chae**[2]

[1]*Department of Chemistry, School of Engineering, University of Petroleum & Energy Studies (UPES), Dehradun - 248007, Uttarakhand, India*
[2]*Advanced Analysis Center, Korea Institute of Science and Technology, Seoul-02792, Republic of Korea*
[3]*School of Agriculture, Dev Bhoomi Uttarakhand University, Dehradun - 248007, Uttarakhand, India*
[4]*Department of Physics, Manav Rachna University, Faridabad, Haryana-121004, India*

(*Received August 27, 2021, Revised June 27, 2022, Accepted August 8, 2022*)

Abstract. Synthesis approaches usually affect the physical and chemical properties of ferrites. This helps ferrite materials to design them for desired applications. Some of these methods are mechanical milling, ultrasonic method, micro-emulsion, co-precipitation, thermal decomposition, hydrothermal, microwave-assisted, sol-gel, etc. These methods are extensively reviewed by taking example of $ZnFe_2O_4$. These methods also affect the microstructure and local structure of ferrite which ultimately affect the physical and chemical properties of ferrites. Various spectroscopic techniques such as Raman spectroscopy, Fourier Transform Infrared spectroscopy, Ultra Violet-Visible spectroscopy, Mössbauer spectroscopy, extended x-ray absorption fine structure, and electron paramagnetic resonance are found helpful to reveal this information. Hence, the basic principle and the usefulness of these techniques to find out appropriate information in $ZnFe_2O_4$ nanoparticles is elaborated in this review.
Keywords: cation occupancy; spectroscopy techniques; synthesis; zinc ferrite nanoparticles

1. Introduction

Ferrite nanoparticles have gained a lot of attention because of their wide applications in numerous appliances such as microelectronics (Kefeni *et al*. 2017), magnetic devices (Pouponneau *et al*. 2009, Kadyrzhanov *et al*. 2019, Pouponneau *et al*. 2009), gas sensing (Godbole *et al*. 2017), adsorbents (Nassar and Khatab 2016, Reddy and Yun 2016, Springer *et al*. 2016), water purification (Girgis *et al*. 2015, Kumar Mukesh *et al*. 2020), catalysis (Kharisov *et al*. 2019), antibacterial activity (Gomes *et al*. 2018), as well as contrast agents in magnetic imaging resonance and biomedical field (Hayek 2019, Ito *et al*. 2005, Gao *et al*. 2009, Hazra and Ghosh 2014). It is well established that these applications depend on the physics and chemistry of ferrites. The chemical and physical properties of ferrite nanoparticles are largely governed by their size, shape, and morphology (Pal *et al*. 2014). A deviation in the size of these nanoparticles can alter the behavior of ferrite without changing composition. Thus, tailoring particle size to get desired physical and chemical properties of ferrite, has become a fascinating field of research and development. So far, various methods of synthesizing spinel ferrite nano-particles have been reported for the production of efficient and high yield nanoparticles with ability of controlling particle size. Some of these methods are hydrothermal (Li *et al*. 2010, Chen *et al*. 2010), co-precipitation (Sivakumar *et al*. 2011, Patange *et al*. 2010), and thermolysis (Bao *et al*. 2007), etc. Various synthesis methods result in different morphology and size of ferrite nanoparticles (Morales-Flores *et al*. 2013, Syahmazgi *et al*. 2014, Rai and Bajpai 2021, Torres *et al*. 2021, Zeng *et al*. 2021) which is responsible for synthesis-dependent physical and chemical behavior of ferrites (Rahman *et al*. 2020, Munir *et al*. 2020). These aspects are covered by many researchers so far, However, less attention is given to investigate micro-structural behavior using spectroscopic techniques. These techniques such as Raman spectroscopy, Fourier transform infrared (FTIR) spectroscopy, UV (ultra voilet)-Vis (Visible) spectroscopy (Lee *et al*. 2013), Mössbauer spectroscopy, extended x-ray absorption fine structure, and electron paramagnetic resonance (EPR) is capable to visualize the insights of the ferrite nanoparticles and reveal the mystery behind various physical properties such as electrical and magnetic properties. Thus, there is need to provide concise and concrete information of these spectroscopic techniques in order to gain in-depth information of ferrite systems. In this review, recent approaches to synthesize ferrite nanoparticles and their characterization by using spectroscopic techniques are elaborated by taking zinc ferrite ($ZnFe_2O_4$) as a prototype material.

2. Synthesis of zinc ferrite nanoparticles

2.1 Mechanical methods

In this method, high-energy shakers/ball mills and sometimes tumbler mills are used. The limitation of this

*Corresponding author, Ph.D.,
E-mail: mamta.latwal@gmail.com
**Co-corresponding author, Ph.D.,
E-mail: khchae@kist.re.kr

ISSN: 2287-237X (Print), 2287-2388 (Online)

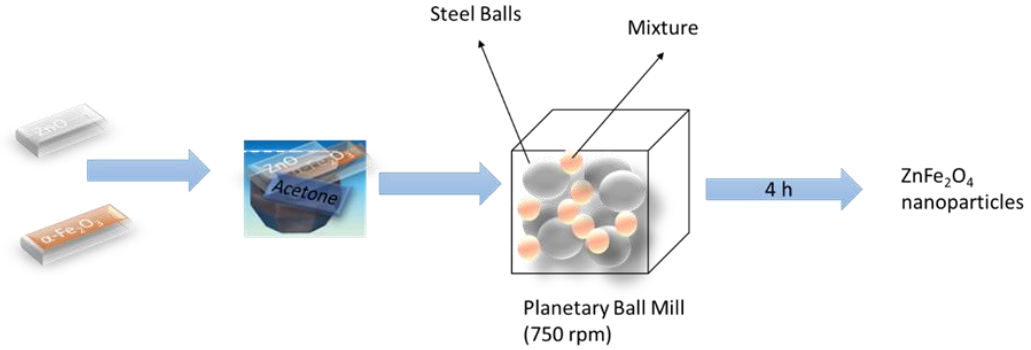

Fig. 1 Mechanical milling of $ZnFe_2O_4$ nanoparticles formation. Redrawn based on the description given by Kim *et al* (Kim and Saito 2001)

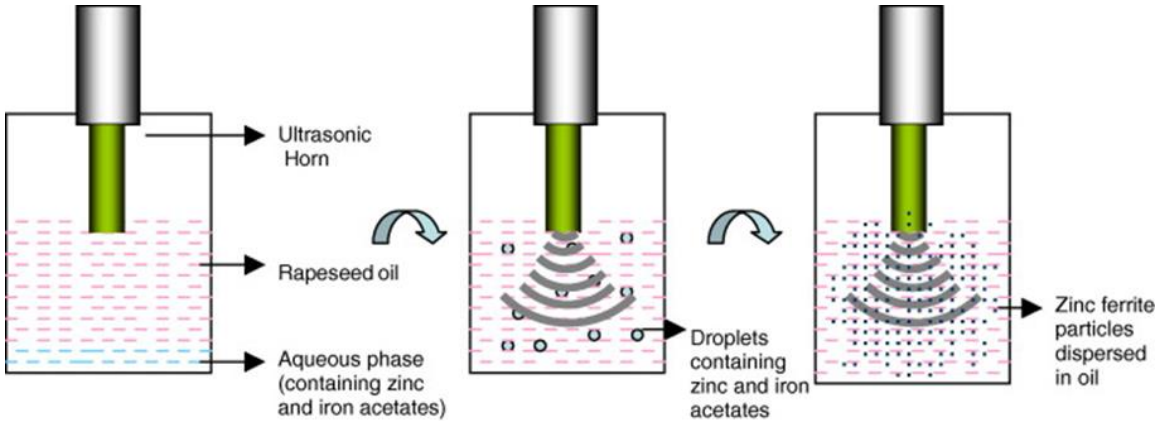

Fig. 2 Schematic representation of ultrasound-mediated techniques for the synthesis of zinc ferrite nanocrystals (Sivakumar *et al*. 2006)

method is the change in the stoichiometry of nanoparticles by the contamination of milling tools during the milling period. Some of the ferrite materials prepared by this technique are zinc ferrite ($ZnFe_2O_4$) (Mozaffari and Masoudi 2014), copper ferrite ($CuFe_2O_4$) (Marinca *et al*. 2012), cobalt ferrite ($CoFe_2O_4$) (Manova *et al*. 2004), nickel ferrite ($NiFe_2O_4$) (Marinca *et al*. 2011, Chen and Zhang 2012), and nickel manganese ferrite ($Ni_{1-x}Mn_xFe_2O_4$) (Todaka *et al*. 2003). Fig. 1 shows the synthesis technique of $ZnFe_2O_4$ nanoparticles by mechanical milling method.

2.2 Ultrasonic method

This method provides control over reaction conditions and particle size distribution. In this method, two major factors that have an impact on the particle size are the temperature and intensity of ultrasonic waves (Yadav *et al*. 2020). Ultrasonication is responsible for the mixing at the atomic level and the formation of the crystalline phase at low temperatures. Some examples are $CuFe_2O_4$ (Abbasian *et al*. 2020), Fe_3O_4 (Lai *et al*. 2004, Goswami *et al*. 2013a), $CoFe_2O_4$ (Goswami *et al*. 2013b), manganese zinc ferrite nanocrystals (Sivakumar *et al*. 2012). $ZnFe_2O_4$ nanocrystals were synthesized by ultrasound-mediated emulsion method using zinc and iron acetates and rapeseed oil shown in Fig. 2 (Sivakumar *et al*. 2006). The method is also able to produce ferrite nanocubes (Yan *et al*. 2015).

2.3 Solvothermal or hydrothermal method

This method is one of the most economical and eco-friendly methods because water is used as a solvent (Gan *et al*. 2020). Nanoparticles of different sizes, shapes, and morphologies can be obtained by controlling the experimental reaction parameters such as temperature, solvent, surfactant, time, and precursor nature. Nanoparticles of Fe_3O_4 (Su *et al*. 2016), $CoFe_2O_4$ (Yáñez-Vilar *et al*. 2009, Allaedini *et al*. 2015), $CuFe_2O_4$, $MnFe_2O_4$, $NiFe_2O_4$ (Tang *et al*. 2012), Ni-Zn ferrite, Co-Ni ferrite, and metal-doped $MgFe_2O_4$ can be synthesized by the solvothermal method (Li *et al*. 2015, Ni *et al*. 2015, Yin *et al*. 2017). This method is also suitable to form ferrite composites (Yao *et al*. 2019). The pristine $ZnFe_2O_4$ nanoparticles were prepared by a hydrothermal route shown in Fig. 3 (Anupriya *et al*. 2021). Preparation of super-paramagnetic $ZnFe_2O_4$ sub-microsphere was carried out by solvothermal method by Ma *et al*. (2017). In this procedure, $FeCl_3.6H_2O$, $ZnCl_2$, CH_3COONa, and glycol were taken in a three-necked flask and mixed for 2 h by continuous stirring. The solution is transferred into an autoclave and heated at 200-215 ºC for 4-8 h. The autoclave was cooled at room temperature for collecting the powder. Prepared nanocrystals were washed with deionized water and ethanol and dried at 60 ºC.

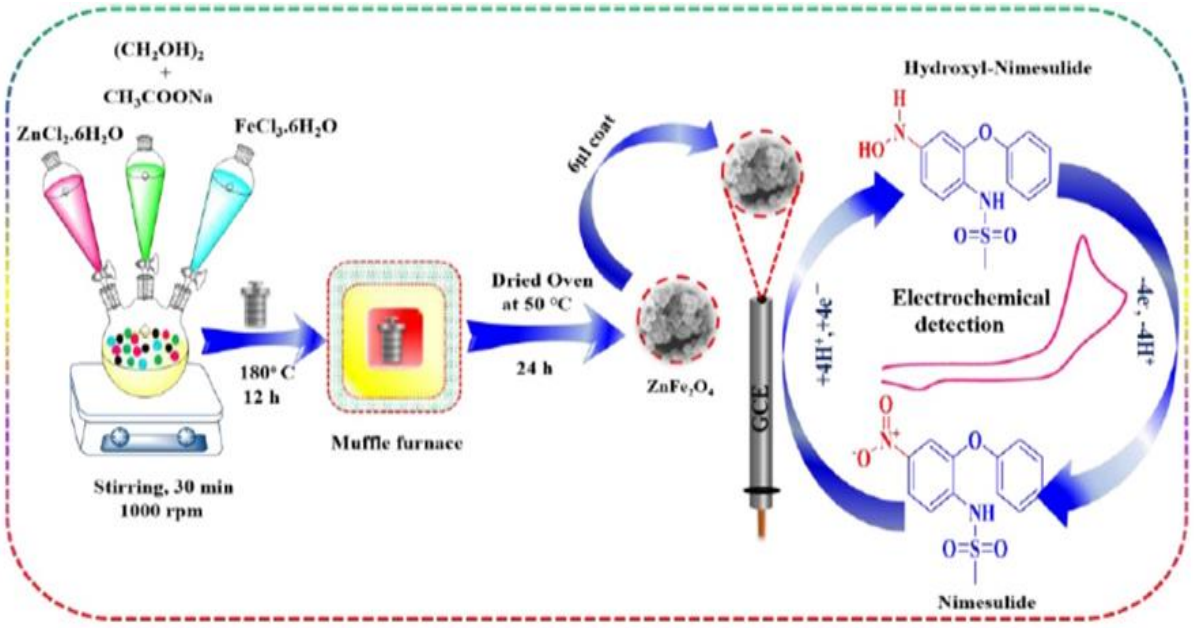

Fig. 3 The schematic diagram for the synthesis procedure and fabrication of the $ZnFe_2O_4$ nanoparticles along with electrochemical mechanism (Anupriya *et al*. 2021)

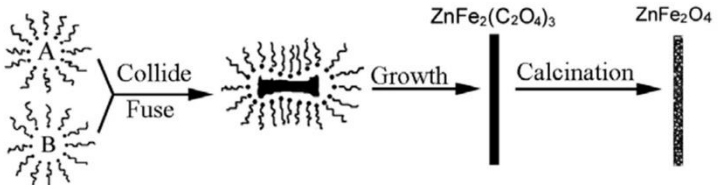

Fig. 4 The schematic diagram for the growth process of porous $ZnFe_2O_4$ nanorods (Zhu *et al*. 2008)

2.4 Microemulsion method

This method is known for its size-controlled nature of the particles. In this method, the two immiscible thermodynamically feasible liquids are stabilized by adding surfactant molecules. This method is environmentally friendly, requires low temperature, and reuses surfactant for several cycles. The main disadvantage of this method is the requirement of a large amount of solvent and prepared particles having poor crystalline nature. Some of the examples are $Mn_{0.5}Zn_{0.5}Fe_2O_4$, $Ni_{0.6}Fe_{2.2}O_4$, Fe_3O_4 (Pang *et al*. 2016, Kefeni *et al*. 2017, Asab *et al*. 2020), barium hexaferrite (Palla *et al*. 1999), neodymium-doped $LiNi_{0.5}Fe_2O_4$ (Gilani *et al*. 2017), and Mn-Zn ferrite nanoparticles (Pemartin *et al*. 2014). The microemulsion method is used to fabricate porous $ZnFe_2O_4$ nanorods with a diameter and length of 50 nm and several micrometers respectively (Fig. 4) (Zhu *et al*. 2008). The microemulsion method for the preparation of ferrite nanoparticles offers a series of advantages due to the possibility to confine reactions into nanosized reactors under the influence of microemulsion properties and dynamics on the control of the shape of nanoparticles discussed. The synthesis procedure evolution by both direct and reverse microemulsions over a selection of ferrite nanoparticles is also described by Scano *et al*. (2019).

2.5 Co-precipitation method

The co-precipitation method is a preferred method to get uniform size particles. Other benefits of this method are less time-consuming, economic, easy to perform, and high mass production. Mixing of the aqueous solution of transition metal salt and the alkaline medium in 1:2 ratios can be done uniformly. The disadvantage of this method is the low crystallinity of the nanoparticles. Various particles such as $CoFe_2O_4$ (Olsson *et al*. 2005, Darwish *et al*. 2019), $MnFe_2O_4$ (Pereira *et al*. 2012, Kurtinaitienė *et al*. 2016, Islam *et al*. 2020), Sn-doped $MnFe_2O_4$, Fe_3O_4 (El Moussaoui *et al*. 2016), $NiFe_2O_4$ (Sagadevan *et al*. 2018), and $Ni_{0.4}Cu_{0.2}Zn_{0.4}Fe_2O_4$ (Peng *et al*. 2021) were prepared by this method. The flow charts for preparing $ZnFe_2O_4$ nanoparticles using the co-precipitation method are elaborated by Andhare *et al*. (2020), (Fig. 5) and Sathiyamurthy *et al*. (2020). In a recent work by Gul *et al*. (2020), this method was adopted to synthesize aluminum doped zinc ferrite for photocatalytic applications.

2.6 Sonochemical method

In this method, microwave energy is used for the combustion of precursors. During the reaction, the microwave energy is converted into thermal energy, and the

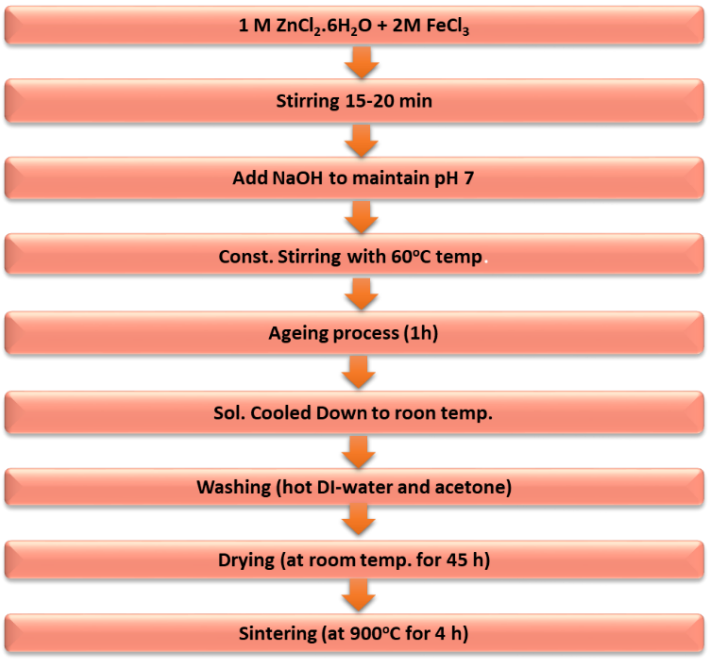

Fig. 5 Flow chart of the synthesis of $ZnFe_2O_4$ nanoparticles prepared by co-precipitation method (a) Andhare *et al*. (2020)

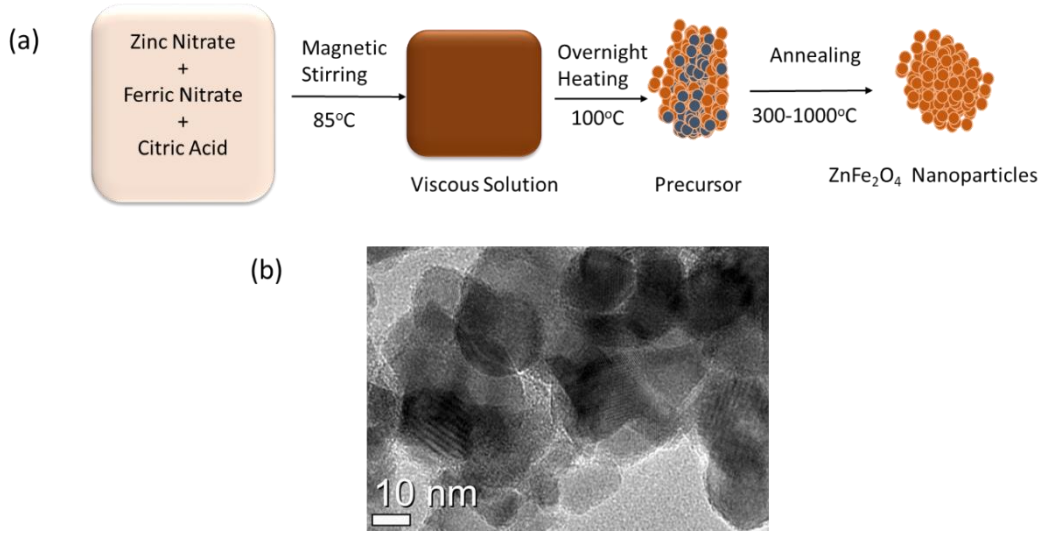

Fig. 6 (a) Flow chart for the formation of zinc ferrite nanoparticles. Redrawn based on the description from (Singh *et al*. 2011a); (b) Transmission electron microscopic image of zinc ferrite nanoparticles by this method

temperature rises from 100 ºC to 200 ºC in a shorter period. The common ferrites prepared by this method are Fe_3O_4, $CoFe_2O_4$ (Kozakova *et al*. 2012, Venkatesh *et al*. 2016), $Mn_{1-x}Ni_xFe_2O_4$, $ZnFe_2O_4$ (Tadjarodi *et al*. 2015, Jesudoss *et al*. 2016, Giridhar *et al*. 2020, Yu *et al*. 2020).

2.7 Sol-gel method

In this method, metal alkoxide solution undergoes hydrolysis and condensation reactions. In the process, the sol is converted into a gel at the end of the reaction. Impurities in the final product can be removed by heat treatment (Gatelytė *et al*. 2011, Zhang and Wu 2013, Shirsath *et al*. 2017, Rashdan and Hazeem 2020). The metal ferrites prepared in this method are $Ni_{0.4}Zn_{0.6-x}Co/Mn_xFe_2O_4$, $MnFe_2O_4$, $NiFe_2O_4$, $CuFe_2O_4$, $ZnFe_2O_4$, etc. (Carta *et al*. 2008b, Mukhtar *et al*. 2015, Sharma *et al*. 2015). $Ni_{0.6}Zn_{0.4}Fe_2O_4$ and $Ni_{0.6}Zn_{0.2}Ce_{0.2}Fe_2O_4$ spinel magnetic nanocubes were fabricated by Hammad *et al*. (2020). An eco-friendly sol-gel method with citrate was used to synthesize the nano-cubic activated nickel-zinc ferrite magnetic nanostructures. The structural and magnetic results showed a high crystallinity in nano-cubes magnetic structure and an enhancement in the total magnetization. A remarkable inhibitory effect on microbes was seen in real sewage samples (Hammad *et al*. 2020). Schematic for the formation of $ZnFe_2O_4$ nanoparticles is shown in Fig. 6(a). Starting materials were taken as zinc nitrate and ferric

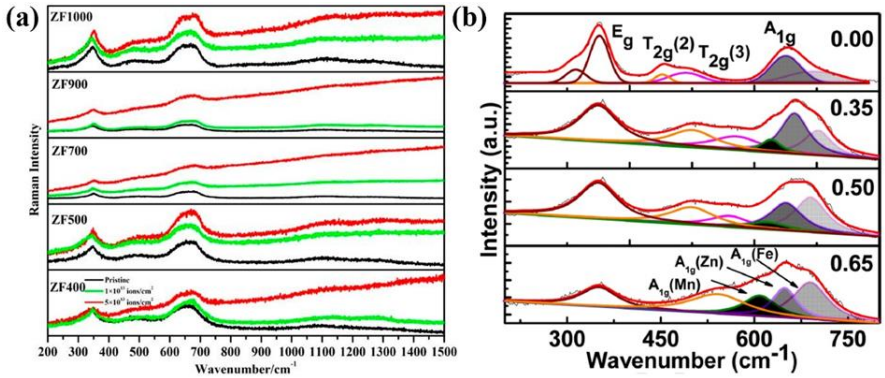

Fig. 7 Raman Spectra of $ZnFe_2O_4$ of (a) different particle sizes (Singh *et al*. 2011c). Permission obtained and (b) doped with different Mn concentrations (Thota *et al*. 2016)

nitrate. Citric acid was used as a host for synthesizing zinc ferrite nanoparticles (Singh *et al*. 2011a, 2016). Fig. 6(b) shows the transmission electron microscopic (TEM) results obtained for the zinc ferrite nanoparticle synthesized at 300ºC (Singh *et al*. 2016). Nanoparticles exhibit clear boundary with well defined shape as can be seen in the TEM image.

2.8 Non-hydrolytic method

High-quality and controlled size nanoparticles are formed by the non-hydrolytic method. Here a suitable organic solvent is used at a high temperature. Well-crystallinity in the nano-particles is formed due to the molecular precursor of organometallic compounds or inorganic-co-ordination complex (Andrianainarivelo *et al*. 1996). This method is called the non-aqueous method because of the formation of nanoparticles as ternary metal-oxides (MFe_2O_4). e.g. $CoFe_2O_4$, $MnFe_2O_4$ (Song and Zhang 2012), and Fe_2O_3 (Li *et al*. 2016). Ferrite nanocrystal was synthesized by a microwave-assisted non-hydrolytic sol-gel process (Bilecka *et al*. 2011). 1 mM of Fe (III) acetyl-acetone was mixed with 5 ml of benzyl alcohol in an inert environment and transferred into a 10 ml glass tube at 170ºC for 12 min. When the reaction was completed, the solution was thermally quenched by compressed air. At last, centrifugation was done and the precipitate was washed with ethanol and diethyl ether and kept for drying. The motor was used to ground powder. The non-hydrolytic coprecipitation method was used for the synthesis of caprylate capped cobalt ferrite nanoparticles (Johnson *et al*. 2020). The particles have a bactericidal effect against *Erwinia carotovora* and *Stenotrophomonas maltophilia*. *The particles responded to the* neodymium magnet with an average particle diameter of 3.81 nm. In addition to these methods, green synthesis methods are also used to grow ferrite nanoparticles (Gokila *et al*. 2021).

3. Spectroscopic methods

3.1 Raman and FTIR spectroscopy

Zinc ferrite which exhibits a cubic spinel structure belongs to the O^7_h (Fd3m) space group. According to the group theory, this space group has the following sets of optical phonon mode at γ point of the Brillouin zone (Fraas and Moore 1972, Singh *et al*. 2013b)

$\Gamma = A_{1g}$ (R) + E_g (R) + F_{1g} + $3F_{2g}$ (R) + $2A_{2u}$ + $2E_u$ + $4F_{1u}$ (IR) + $2F_{2u}$

There are five first-order Raman active modes ($A_{1g} + E_g + 3F_{2g}$). The bands corresponding to these modes are observed at ambient conditions in the Raman spectrum of $ZnFe_2O_4$ as follows: $T_{2g}/F_{2g}(1) = 221$ cm^{-1}, E_g = 246 cm^{-1}, $T_{2g}/F_{2g}(2) = 355$ cm^{-1}, $F_{2g}(3) = 451$ cm^{-1} and E_g = 647 cm^{-1}.

In the Raman spectrum of any ferrite, the bands above 600 cm^{-1} mostly correspond to the motion of oxygen in the tetrahedral AO_4 group (Wang *et al*. 2002) while other low-frequency bands represent the characteristics of the octahedral BO_6 site. Fig. 7(a) shows the typical Raman spectrum of $ZnFe_2O_4$ (ZF) nanoparticles synthesized using different annealing temperatures 400 (ZF400), 500 (ZF500), 700 (ZF700), 900 (ZF900), and 1000 ºC (ZF1000) in the effect of 100 MeV O^{7+} ions under the fluence of 1×10^{13} and 5×10^{13} ions/cm^2 (Singh *et al*. 2011c). The Raman spectra of $ZnFe_2O_4$ show peaks appearing at 452 and 490 cm^{-1} corresponding to T_{2g} (2) and T_{2g} (3), respectively (Fig. 7(b)). It may be noted that both of these modes shift towards the higher wavenumber as the Zn is substituted by Mn in $Mn_xZn_{1-x}Fe_2O_4$ ferrite. The shift in the frequency of these modes strongly suggests that Mn substituted Zn ferrites possess spinel structure lying between normal and inverse.

In the above equation, the four F_{1u} modes (ν_1, ν_2, ν_3, and ν_4) are infrared active, hence bands corresponding to these modes are observed in the FTIR spectrum (Fig. 8). The high-frequency bands ~549–555 cm^{-1} and 422–383 cm^{-1} in FTIR spectrum are corresponding to modes ν_1 and ν_2 respectively. The presence of these bands is attributed to the stretching vibration of Fe^{3+} in both tetrahedral and octahedral positions, respectively. The third vibrational frequency mode ν_3, (370-325 cm^{-1}) is associated with the divalent octahedral metal ions and oxygen complexes. The fourth vibrational mode, ν_4, (280-246 cm^{-1}) is attributed to the lattice vibrational frequency (Ahmed *et al*. 2002). Fig. 8(a) shows the FTIR analysis of the as-prepared and annealed zinc ferrite by Khalili and Farahmandjou (2020).

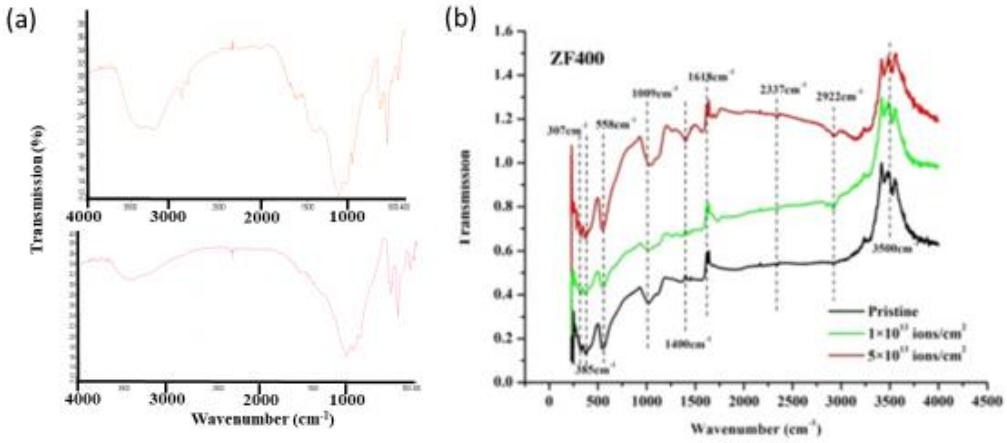

Fig. 8 FTIR spectra of as-prepared (upper panel) and annealed Zinc ferrite samples (lower panel) (Khalili Farahmandjou 2020); (b) FTIR Spectra of $ZnFe_2O_4$ nanoparticles under the fluence of 1×10^{13} and 5×10^{13} ions/cm^2 of 100 MeV O^{7+} (Singh *et al*. 2013c)

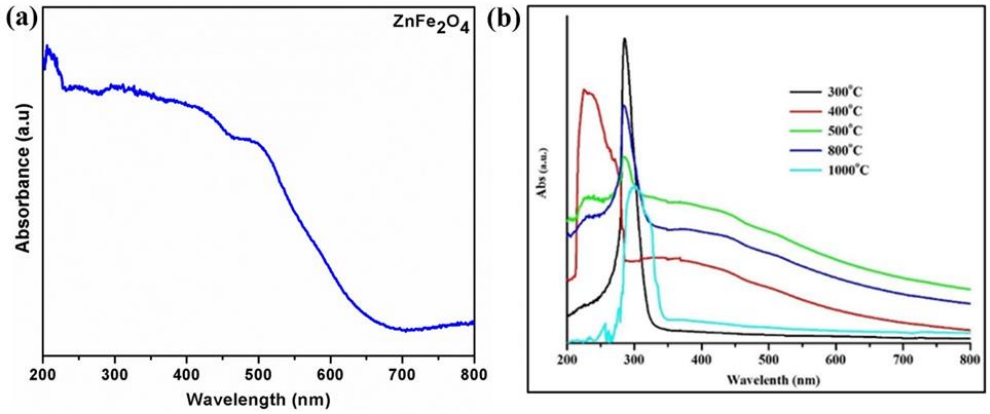

Fig. 9 (a) UV-Vis absorbance spectra of zinc ferrite nanoparticles (Ramachandran and Vishista 2014); (b) UV-Vis absorption spectra of $ZnFe_2O_4$ sintered at different temperatures (Singh *et al*. 2010)

Fig. 8(b) shows the FTIR spectra of zinc ferrite (ZF400) in the effect of 100 MeV O^{7+} ions under the fluence of 1×10^{13} and 5×10^{13} ions/cm^2 (Singh *et al*. 2013c). The bands appearing above 3000 cm^{-1} are due to absorbed moisture from environment (Busca *et al*. 1993).

3.2 UV-Vis spectroscopy

Fig. 9(a) shows the UV-Vis spectra of zinc ferrite synthesized by Ramachandran and Vishista (2014). In Fig. 9(b), UV-Vis for zinc ferrite synthesized under different annealing temperatures ranging from 300 to 1000 °C is shown (Singh *et al*. 2010). In both cases, three distinct regions in the UV-Vis absorption spectra can be easily identified: (1) weak absorption tail, which originates from defects and impurities, (2) exponential edge region, related to the structural randomness, and (3) high absorption region that determines the optical band-gap (Tauc 1974, Urbach 1953). The spectrum shows strong absorption in the UV region, which is a characteristic feature of ferrite materials (Muret 1974). The absorption spectra of these samples reflect the smooth absorption spectra in the wavelength range from 300 to 400 nm. This is attributed to the $3d^5$ – $3d^4 4s^1$ transition of Fe^{3+} ions (Tanaka *et al*. 2006).

In high absorption region, the transition can be characterized by the following relation (Tauc and Menth 1972, Fox and Bertsch 2002, Joshi *et al*. 2003)

$\alpha h\vartheta = A(h\vartheta - E_g)^n, \alpha = \frac{2.303Abs}{t}$ where, A is a constant, E_g is the energy bandgap of the material, n is an index showing the nature of the transition. n = 1/2, 2, 3/2, or 3 for allowed direct, allowed indirect, forbidden direct, and forbidden indirect electronic transitions respectively. Estimation of the bandgap is done by plotting a curve between $(\alpha h\nu)^{1/n}$ and hν. Optical band-gap values can be obtained by extrapolating the curve to the hν-axis. Fig. 10(a) shows the representative $(\alpha h\nu)^2$ *vs* hν plot and its extrapolation to a straight line. This estimates a value of an optical band gap of 2.4 eV (Ramachandran and Vishista 2014). The estimated bandgap of the nanosized zinc ferrite as a function of annealing temperature is shown in Fig. 10(b). The values of the bandgap are of the order of 4.0 eV and correspond to n = 1/2 transitions (Singh *et al*. 2010). The variation of optical band-gap with annealing temperature is explained by Singh *et al*. (2010) based on the existing theories (Schmitt-Rink *et al*. 1987, Zhi-hao *et al*. 2008).

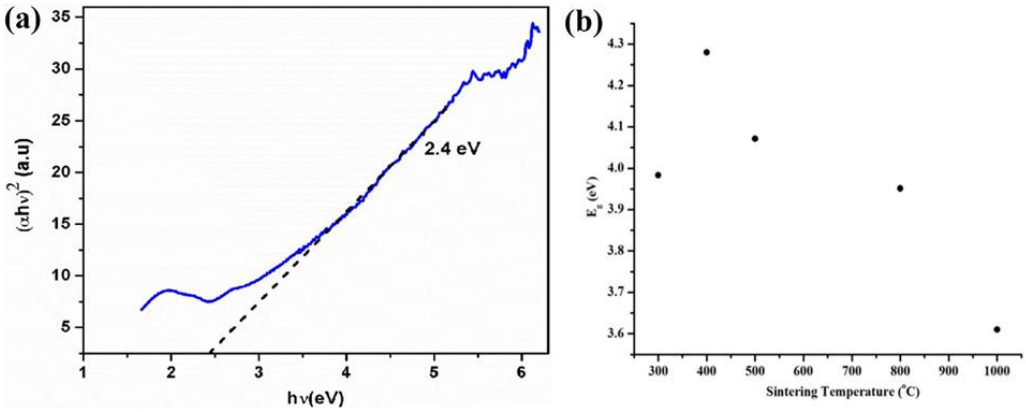

Fig. 10 (a) $(\alpha h\upsilon)^2$ *vs* hυ plot for the samples sintered at 300 °C (Ramachandran and Vishista 2014); (b) Optical band-gap as a function of sintering temperature (Singh *et al*. 2010)

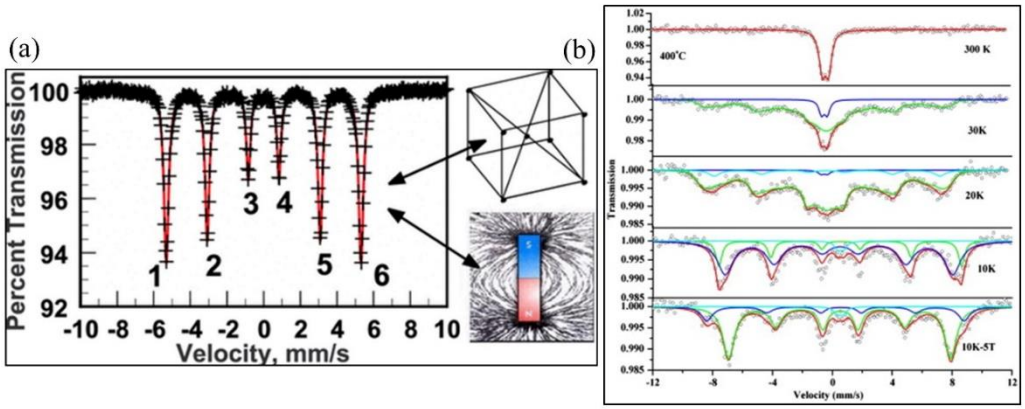

Fig. 11 (a) Mössbauer spectroscopy of Iron (Grandjean and Long 2021); (b) In-field and variable temperature Mössbauer spectra of the samples sintered at 400 °C (Singh *et al*. 2012)

3.3 Mössbauer spectroscopy

This technique responds to the radioactive ^{57}Fe present in ferrites. Pure body-centered cubic (bcc) iron is magnetic at room temperature. There is no electric quadrupole splitting due to the symmetry. The Mössbuaer spectrum of Fe consists of a sextet (Fig. 11(a)) (Grandjean and Long 2021). The sextet in the spectrum is due to 6 nuclear transitions which are allowed by the magnetic dipole selection rule. Note that it is symmetric, but its center of symmetry has an offset from v = 0 (caused by the isomer shift) (Bhide 1973). The hyperfine magnetic field of bcc Fe at room temperature is 310 kG. The selection rule for magnetic dipole transitions restricts transitions to ΔM = 0, ±1.

The relative intensities among peaks are determined by the state of the magnetic field in the sample. For a sample of isotropic magnetic field distribution, the relative intensities of the six peaks are

$$I_1 : I_2 : I_3 : I_4 : I_5 : I_6 = 3 : 2 : 1 : 1 : 2 : 3$$

Though, nanosized $ZnFe_2O_4$ exhibits either super-paramagnetic at room temperature (Fig. 11(b)), however, the double sextet is observed due to the presence of Fe ions at *A* and *B*-sites at low temperature (Singh *et al*. 2012).

The area ratio of sextet corresponding to *A*-site and *B*-site is utilized to estimate cation inversion using the following relation (Kumar Hemaunt *et al*. 2016)

$\frac{x}{1-x} = \frac{I_A}{I_B}$ where, I_A and I_B are the areas of sextet corresponding to *A* and *B*-site, respectively. To date, this technique is suitable to estimate the cation inversion in ferrite nanoparticles and is successfully applied to $ZnFe_2O_4$ by several researchers (Upadhyay and Verma 2004, Lazarević *et al*. 2014). The obtained Mössbauer spectrum is simulated using simulation packages like MOSPLAV (Chipaux 1990), SpectrRelax (Matsnev and Rusakov 2012), and MossWinn (Klencsár *et al*. 1996). NORMOS is one of the widely used simulation packages in ferrite materials (Kumar *et al*. 2017). $ZnFe_2O_4$ nanoparticles synthesized by mechanical method show a typical superparamagnetic-like behavior at room temperature as determined from this spectroscopy (Nachbaur *et al*. 2009). $ZnFe_2O_4$ nanoparticles of crystallite size 10 nm synthesized using high-energy ball-milling from a powder mixture of zinc oxide (ZnO) and hematite (α-Fe_2O_3 exhibits formula $(Zn_{0.31}^{2+}Fe_{0.69}^{3+})_A(Zn_{0.69}^{2+}Fe_{1.31}^{3+})_BO_4^{2-}$ (Ammar *et al*. 2001). The onset of cation inversion was also observed in $ZnFe_2O_4$ when synthesized using the microemulsion method (Ahn *et al*. 2002), and aerogel procedure (Sivakumar *et al*. 2012). Mössbauer spectra of combustion synthesized $NiFe_2O_4$ nanoparticles relate to the occupancy of different numbers

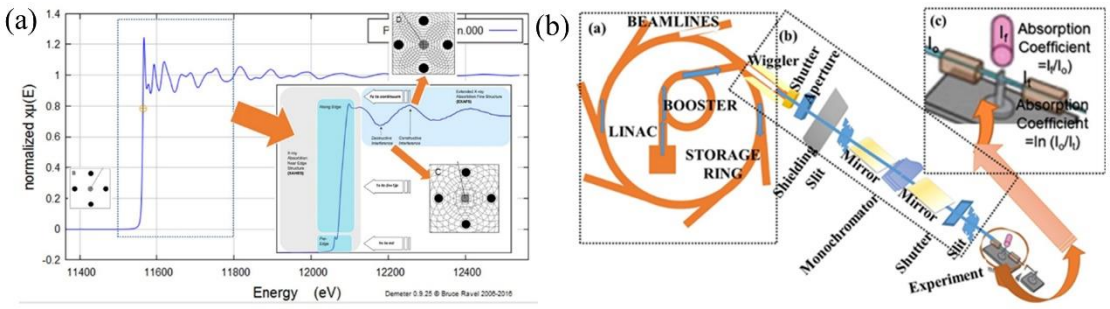

Fig. 12 (a) A typical EXAFS spectrum of material. The various region and their physical interpretation are also depicted; (b) A schematic experimental setup for measuring the EXAFS spectrum

of Ni^{2+} cations at Fe^{3+} tetrahedral and octahedral sites (Ushakov *et al*. 2017). Mössbauer spectroscopy studies on sol-gel synthesized Ce doped $CoFe_2O_4$ nanoparticles confirm the magnetic order with increasing super-paramagnetic contribution and cation distribution showing partial inverse spinel structure (Hashhash *et al*. 2020). Though this technique is superior to others, it has the following drawbacks (Cohen 1976)

(i) It is sensitive to ^{57}Fe, which is only 2% of Fe, Thus, a large amount of sample is required for measurements.

(ii) Measurement time is usually longer around 10-12 h. In addition to this deposition of ^{57}Fe layer is required along with $ZnFe_2O_4$.

(iii) Distribution of Zn^{2+} cannot be determined. It is assumed based on the distribution of Fe^{3+} ions in the system.

(iv) It cannot determine cation redistribution in the case of paramagnetic/superparamagnetic states.

Thus, any technique which does not depend on the magnetic state of metal ferrites for the determination of cation redistribution will be much informative. This techniques is discussed in next section.

3.4 Extended X-ray absorption fine structure (EXAFS) Measurements

These measurements do not only help to understand the cation inversion but also provide information about coordination numbers and metal-oxygen bond length in a tetrahedral and octahedral environment. These measurements are successfully applied to ferrite nanoparticles (Chinnasamy *et al*. 2007, Upadhyay *et al*. 2007, Carta *et al*. 2008a). Cation occupancies are investigated in Mg, Co, Ni, Zn, and Al ferrite nanoparticles by this technique (Henderson *et al*. 2007, Akhtar *et al*. 2009). The detailed information on this technique is depicted elsewhere and can be found in the recent chapter from our group (Sharma *et al*. 2018). Fig. 12(a) depicts the EXAFS spectrum for Pt foil showing the origin of various regions.

The EXAFS spectrum is depicted by the EXAFS equation shown below (Sharma *et al*. 2018)

$$\chi(k) = \sum_z \frac{N_z S_0^2 f_z(k)}{kR_z^2} e^{-2k^2\sigma_z^2} e^{-2R_z/\lambda_z(k)} \sin[2kR_z + \delta_z(k)]$$

where N_z denotes the total number of atoms in the z^{th} shell, λ_z is the mean-free path of photoelectron and f_z is the backscattering amplitude. σ_z which is the fluctuation in R_z due to structural disorder and temperature. Sin $[2kR_z+\delta_z(k)]$ represents oscillations in the EXAFS spectrum and $\delta_z(k)$ is the phase shift. S_0^2 is known as the amplitude reduction factor. k is wave-vector and $\chi(k)$ is the absorption coefficient. Since wave vector is related to the energy of X-ray photon, hence, EXAFS spectrum in Fig. 12(a) is plotted as a variation between the absorption coefficient and photon energy.

EXAFS measurements are generally performed by using synchrotron radiation which is produced by the accelerators based on a storage ring (Basu *et al*. 2014). One of the major sources of synchrotron radiation is Pohang Accelerator Laboratory, Pohang, South Korea (Aquilanti *et al*. 2015). This laboratory comprises almost 24 beamlines. 1D KIST (Korea Institute of Science and Technology) beamline is utilized for measuring EXAFS (Parc *et al*. 2009). A description of the storage ring, beamline, and measuring EXAFS spectrum is depicted in Fig. 12(b).

The measured EXAFS spectrum is normalized and converted to momentum space from energy space using ATHENA. Thus, obtained spectrum is Fourier transformed to radial (R) space. The quantitative information of cation redistribution is obtained by simulating the spectrum using the ARTEMIS program (Lee *et al*. 2010). Thus, several researchers utilized this technique to estimate cation occupancies in ferrite nanoparticles (Oliver *et al*. 2000, Calvin *et al*. 2002, Ravel and Newville 2005, Nakashima *et al*. 2007, Gomes *et al*. 2011). In zinc ferrite, super-occupation of Fe^{3+} ions at tetrahedral sites without Zn^{2+} inversion was established under certain conditions (Gomes *et al*. 2011). The non-equilibrium cation site occupancy in nano-sized $ZnFe_2O_4$ (~6–13 nm) with different degrees of inversion (~0.2 to 0.4) was investigated using Fe and Zn *K*-edge XANES and EXAFS measurements (Oliver *et al*. 2000). In our group, an attempt was made to determine cation occupancies in zinc ferrite. For this purpose, a zinc ferrite sputtering target was procured from Alfa Aesar, and the Fe *K*-edge EXAFS spectrum is measured as shown in Fig. 13(a). Fig. 13(b) shows the simulated Fourier transform of EXAFS spectra at the Fe *K*-edge of this material. This shows that almost 9% of Fe atoms reside on the A-site.

In addition, these measurements can inform any change of valence state and hybridization in ferrite nanoparticles (Stewart *et al*. 2007, Singh *et al*. 2016, 2018). The main drawback of this technique is that no information of magnetic order can be obtained.

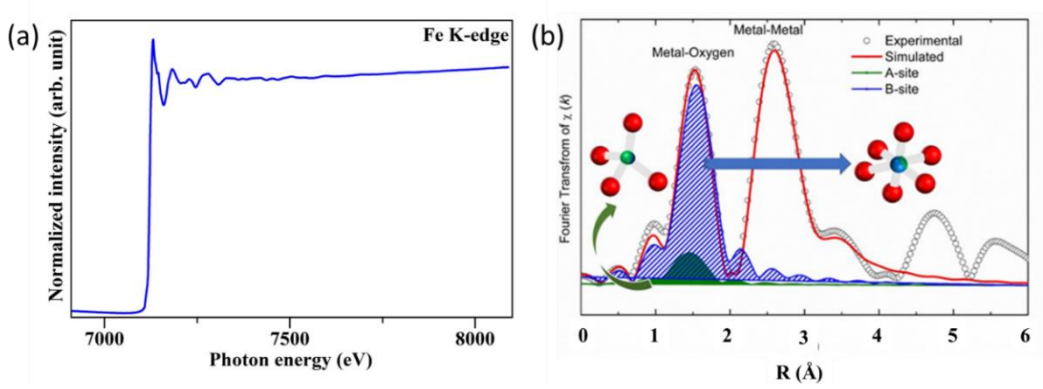

Fig. 13 (a) A typical EXAFS spectrum of $ZnFe_2O_4$; (b) Fourier transform of EXAFS spectrum of zinc ferrite sputtering target at Fe *K*-edge. R-oscillations at 1.7 and 2.9 Å represent metal-oxygen and metal-metal interaction. Schematic of A-site and B-site are shown to represent occupancies Zn^{2+} ion (green) and Fe^{3+} ions at these sites

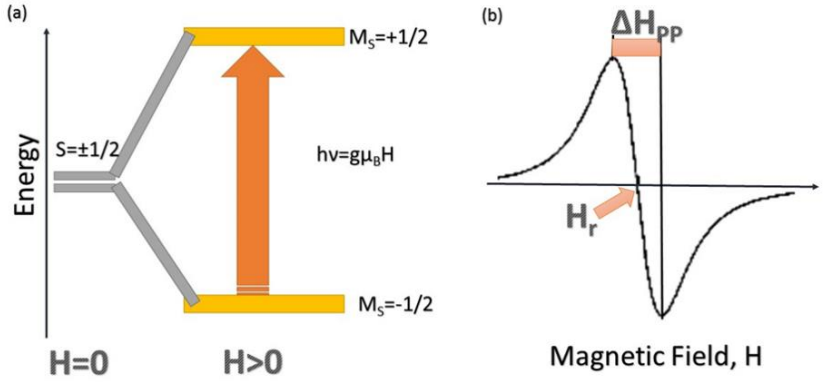

Fig. 14 Principle of electron paramagnetic resonance: (a) spin energy levels under magnetic field and (b) Spectrum showing peak to peak line-width (ΔH_{pp}) and resonance field (H_r) of electron paramagnetic resonance spectrum.

3.5 Electron paramagnetic resonance (EPR) Spectroscopy

EPR studies the interaction between the electron's magnetic moments and the magnetic fields. The EPR has its base on the extension of the Stern-Gerlach experiment which showed that an atom with a net magnetic moment can take up only discrete orientations in a magnetic field. Electrons have two orientations corresponding to two different spin energy states (i) (S_z = +1/2ħ), which corresponds to higher energy states, and (ii) (S_z = –1/2 ħ) which corresponds to lower energy states. The energy difference between these two states is thus given by (Parmar *et al*. 2015)

$$\Delta E = g\mu_B H$$

Resonance takes place when radiation of frequency ω_o is provided such that

$$\Delta E = \hbar\omega_0 = g\mu_B H$$

From this equation, resonance takes place only in the presence of a static magnetic field H. This requirement is a unique aspect of magnetic resonance (Fig. 14).

The information about the line-position is given by g-value, which was estimated by using $g = 2.00367\frac{H_{DPPH}}{H_r}$ where H_r in the original absorption curve is the field corresponding to absorption (i.e., resonance field) for the given sample. H_{DPPH} is the resonance field corresponding to the diphenyl picrylhydrazyl (DPPH) marker. Thus, this technique was utilized by our group to investigate magnetic interaction in zinc ferrite nanoparticles based on parameters like g-value and peak to the peak line width (Murphy 2008, Singh *et al*. 2008). The drastic change in these parameters for the zinc ferrite nanoparticle after irradiation may be attributed to the irradiation-induced anisotropy of the magnetic moment due to the splitting of crystallites and change in the shape of particles (Singh *et al*. 2009). The variation of g-values and peak-to-peak linewidth with temperature envisages different values of activation energies of the spins in zinc ferrite nanoparticles of two different sizes (Singh *et al*. 2011a). Further, the change in *g*-values of pristine and irradiated specimens shows the attributes of cation inversion after irradiation (Singh *et al*. 2013a, Singh *et al*. 2014). This technique is also effective to elaborate the preferential orientation of grains in zinc ferrite thin films (Singh *et al*. 2011b).

4. Conclusions

In conclusion, various synthesis techniques for preparing

zinc ferrite nanoparticles are discussed. Spectroscopic techniques to characterize these nanoparticles are also included in this review. Techniques such as Raman and FTIR spectroscopy give microstructural information. However, UV-vis spectroscopy determines the optical behavior of ferrites by depicting nature of transition.The quantitative information of cation redistribution is determined using Mössbauer spectroscopy and extended X-ray absorption fine structure measurements. The spin-canting effects in metal ferrite nanoparticles are determined using in-field Mössbauer spectroscopy. The electron paramagnetic resonance spectroscopy depicts the nature of exchange interaction. Overall this article provides detailed information on the synthesis and spectroscopic techniques of ferrite nanoparticles.

Acknowledgments

KHC acknowledges the financial support received through the Korea Institute of Science and Technology (KIST 2V09190). JPS acknowledges Science and Engineering Research Board (SERB), New Delhi for providing Ramanujan Fellowship. JPS is thankful to Hon'ble Vice Chancellor, Manav Rachna Univeristy, Faridabad for extending UV and FTIR spectroscopic facilities at University Instrumentation Centre (UIC).

References

Abbasian, A., Hosseini, S., Shayesteh, M., Shafiee, M. and Esmaeilzaei M.R. (2020), "Ultrasonic-assisted solvothermal synthesis of self-assembled copper ferrite nanoparticles", *Int. J. Nano Dimension*, **11**(2), 130-144.

Ahmed, M.A., Ateia, E. and El-Dek, S.I. (2002), "Spectroscopic analysis of ferrite doped with different rare earth elements", *Vib. Spectrosc.*, **30**(1), 69-75. https://doi.org/10.1016/S0924-2031(02)00040-1.

Ahn, Y., Choi, E.J., Kim, S., An, D.H., Kang, K.U., Lee, B.G., Baek, K.S. and Oak, H.N. (2002), "Magnetization and Mossbauer study of nanosize $ZnFe_2O_4$ particles synthesized by using a microemulsion method", *J. Korean Phys. Soc.*, **41**(1), 123-128.

Akhtar, M.J., Nadeem, M., Javaid, S. and Atif, M. (2009), "Cation distribution in nanocrystalline $ZnFe_2O_4$ investigated using x-ray absorption fine structure spectroscopy", *J. Phys. Condens. Matter*, **21**(40), 405303. https://doi.org/10.1088/0953-8984/21/40/405303.

Allaedini, G., Tasirin, S. M. and Aminayi, P. (2015), "Magnetic properties of cobalt ferrite synthesized by hydrothermal method", *Int. Nano Lett.*, **5**(4), 183-186. https://doi.org/10.1007/s40089-015-0153-8.

Ammar, S., Helfen, A., Jouini, N., Fiévet, F., Rosenman, I., Villain, F., Molinié, P. and Danot, M. (2001), "Magnetic properties of ultrafine cobalt ferrite particles synthesized by hydrolysis in a polyol medium", *J. Mater. Chem.*, **11**(1), 186-192. https://doi.org/10.1039/B003193N.

Andhare, D.D., Jadhav, S.A., Khedkar, M.V., Somvanshi, S.B., More, S.D. and Jadhav, K.M. (2020), "Structural and chemical properties of $ZnFe_2O_4$ nanoparticles synthesised by chemical co-precipitation technique", *J. Phys. Conference Series*, **1644**, 012014. https://doi.org/10.1088/1742-6596/1644/1/012014.

Andrianainarivelo, M., Corriu, R., Leclercq, D., Mutin, P. H. and Vioux, A. (1996), "Mixed oxides SiO_2–ZrO_2 and SiO_2–TiO_2 by a non-hydrolytic sol–gel route", *J. Mater. Chem.*, **6**(10), 1665-1671. https://doi.org/10.1039/JM9960601665.

Anupriya, J., Babulal, S.M., Chen, T.W., Chen, S.M., Kumar, J.V., Lee, J.W., Rwei, S.P., Yu, J., Yu, R. and Hong, C.Y. (2021), "Facile hydrothermal synthesis of cubic zinc ferrite nanoparticles for electrochemical detection of antiinflammatory drug nimesulide in biological and pharmaceutical sample", *Int. J. Electrochem. Sci.*, **16**, 1-19. https://doi.org/10.20964/2021.07.72.

Aquilanti, G., Vaccari, L., Plaisier, J.R. and Goldoni, A. (2015), *Instrumentation at Synchrotron Radiation Beamlines*, In *Synchrotron Radiation: Basics, Methods and Applications*, Springer Berlin Heidelberg, Berlin, Heidelberg.

Asab, G., Zereffa, E. A. and Seghne, T. A. (2020), "Synthesis of silica-coated Fe_3O_4 nanoparticles by microemulsion method: characterization and evaluation of antimicrobial activity", *Int. J. Biomater.*, **2020**, 1-11. https://doi.org/10.1155/2020/4783612

Bao, N., Shen, L., Wang, Y., Padhan, P. and Gupta, A. (2007), "A facile thermolysis route to monodisperse ferrite nanocrystals", *J. Am. Chem. Soc.*, **129**(41), 12374-12375. https://doi.org/10.1021/ja074458d.

Bhide, V.G. (1973), *Mössbauer Effect and Its Applications*, Tata McGraw-Hill Pub. Co., New Delhi, India.

Basu, S., Nayak, C., Yadav, A.K. Agrawal, A., Poswal, A.K. Bhattacharyya, D., Jha, S.N. and Sahoo, N.K. (2014), "A comprehensive facility for EXAFS measurements at the INDUS-2 synchrotron source at RRCAT, Indore, India", *J. Phys.*, **493**, 012032.

Bilecka, I., Kubli, Amstad, M. E. and Niederberger, M. (2011), "Simultaneous formation of ferrite nanocrystals and deposition of thin films via a microwave-assisted nonaqueous sol–gel process", *J. Sol-Gel Sci. Technol.*, **57**, 313-322. https://doi.org/10.1007/s10971-010-2165-1.

Busca, G., Lorentzelle, V., Ramis, G. and Willey, R.J. (1993), *Langmuir*, **9**, 1402.

Calvin, S., Carpenter, E.E. , Ravel, B., Harris, V.G. and Morrison, S.A. (2002), "Multiedge refinement of extended x-ray-absorption fine structure of manganese zinc ferrite nanoparticles", *Phys. Rev. B*, **66**(22), 224405. https://doi.org/10.1103/PhysRevB.66.224405.

Carta, D., Casula, M. F., Mountjoy, G. and Corrias, A. (2008a), "Formation and cation distribution in supported manganese ferrite nanoparticles: an x-ray absorption study", *Phys. Chem. Chem. Phys.*, **10**(21), 3108-3117. https://doi.org/10.1039/B800359A.

Carta, D., Loche, D., Mountjoy, G., Navarra, G. and Corrias, A. (2008b), "$NiFe_2O_4$ nanoparticles dispersed in an aerogel silica matrix: an x-ray absorption study", *J. Phys. Chem. C*, **112**(40), 15623-15630. https://doi.org/10.1021/jp803982k.

Chen, D. and Zhang, Y.Z. (2012), "Synthesis of $NiFe_2O_4$ nanoparticles by a low temperature microwave-assisted ball milling technique", *Sci. China Technol. Sci.*, **55**(6), 1535-1538. https://doi.org/10.1007/S11431-012-4772-2.

Chen, L., Dai, H., Shen, Y. and Bai, J. (2010), "Size-controlled synthesis and magnetic properties of $NiFe_2O_4$ hollow nanospheres via a gel-assistant hydrothermal route", *J. Alloys Compd.*, **491**(1), L33-L38. https://doi.org/10.1016/j.jallcom.2009.11.031.

Chinnasamy, C.N., Yang, A., Yoon, S.D., Hsu, K., Shultz, M.D., Carpenter, E.E., Mukerjee, S., Vittoria, C. and Harris, V.G. (2007), "Size dependent magnetic properties and cation inversion in chemically synthesized $MnFe_2O_4$ nanoparticles", *J. Appl. Phys.*, **101**(9), 09M509. https://doi.org/10.1063/1.2710218.

Chipaux, R. (1990), "MOSPLV, a program for simulation of complex Mössbauer spectra in polycrystalline samples", *Comput. Phys. Commun.*, **60**(3), 405-415.

https://doi.org/10.1016/0010-4655(90)90037-2.

Cohen, R.L. (1976), *Elements of Mossbauer Spectroscopy*, In *Applications of Mossbauer spectroscopy*, Academic Press: New York, U.S.A.

Darwish, M.S., Kim, H., Lee, H., Ryu, C., Lee, J.Y. and Yoon, J. (2019), "Synthesis of magnetic ferrite nanoparticles with high hyperthermia performance via a controlled co-precipitation method", *Nanomaterials*, **9**(8), 1176. https://doi.org/10.3390/nano9081176.

El Moussaoui, H., Mahfoud, T., Habouti, S., El Maalam, K., Ali, B.M., Hamedoun, M., Mounkachi, O., Masrour, R., Hlil, E.K. and Benyoussef, A. (2016), "Synthesis and magnetic properties of tin spinel ferrites doped manganese", *J. Magn. Magn. Mater.*, **405**, 181-186. https://doi.org/10.1016/j.jmmm.2015.12.059.

Fox, M. and Bertsch, G.F. (2002), "Optical properties of solids", *Am. Assoc. Phys. Teachers*, **70**, 1269.

Fraas, L.M. and Moore, J.E. (1972), "Raman selection rule violation for a spinel crystal", *Rev. Bras. Educ. Fís.*, **2**(3), 299.

Gan, Y.X., Jayatissa, A.H., Yu, Z., Chen, X. and Li, M. (2020), "Hydrothermal synthesis of nanomaterials", *J. Nanomater.*, **2020**, 8917013. https://doi.org/10.1155/2020/8917013.

Gao, J., Gu, H. and Xu, B. (2009), "Multifunctional magnetic nanoparticles: design, synthesis, and biomedical applications", *Accounts Chem. Res.*, **42**(8), 1097-1107. https://doi.org/10.1021/ar9000026.

Gatelytė, A., Jasaitis, D., Beganskienė, A. and Kareiva, A. (2011), "Sol-gel synthesis and characterization of selected transition metal nano-ferrites", *Mater. Sci.*, **17**(3), 302-307. https://doi.org/10.5755/j01.ms.17.3.598.

Gilani, Z.A., Anjum, M.N., Shifa, S., Asghar, H.M.N.U.H.K., Rehman, J.U., Usmani, M.N., Aslam, S., Khan, M.A., Shahid, M. and Warsi, M.F. (2017), "Morphological and magnetic behavior of neodymium doped $LiNi_{0.5}Fe_2O_4$ nanocrystalline ferrites prepared via micro-emulsion technique", *Digest J. Nanomater. Biostruct.*, **12**(1), 223-228. https://doi.org/10.1023/A:1010004616528.

Girgis, E., Adel, D., Tharwat, C., Attallah, O. and Rao, K.V. (2015), "Cobalt ferrite nanotubes and porous nanorods for dye removal", *Adv. Nano Res.*, **3**(2), 111. http://doi.org/10.12989/anr.2015.3.2.111.

Giridhar, M., Naik, H.S.B., Sudhamani, C.N., Prabakara, M.C., Kenchappa, R., Venugopal, N. and Patil, S. (2020), "Microwave-assisted synthesis of water-soluble styrylpyridine dye-capped zinc oxide nanoparticles for antibacterial applications", *J. Chin. Chem. Soc.*, **67**(2), 316-323. https://doi.org/10.1002/jccs.201900029.

Godbole, R., Rao, P. and Bhagwat, S. (2017), "Magnesium ferrite nanoparticles: A rapid gas sensor for alcohol", *Mater. Res. Express*, **4**(2), 025032. https://doi.org/10.1088/2053-1591/aa5ec7.

Gokila, V., Perarasu, V. and Rufina, R.D.J. (2021), "Qualitative comparison of chemical and green synthesized Fe_3O_4 nanoparticles", *Adv. Nano Res.*, **10**(1), 71. http://doi.org/10.12989/anr.2021.10.1.071.

Gomes, G.A., Costa, G.L.D. and da Silva Figueiredo, A.B.H. (2018), "Synthesis of ferrite nanoparticles $Cu_{1-x}Ag_xFe_2O_4$ and evaluation of potential antibacterial activity", *J. Mater. Res. Technol.*, **7**(3), 381-386. https://doi.org/10.1016/j.jmrt.2018.04.021.

Gomes, J.A., Azevedo, G.M., Depeyrot, J., Mestnik-Filho, J., da Silva, G.J., Tourinho, F.A. and Perzynski, R. (2011), "$ZnFe_2O_4$ nanoparticles for ferrofluids: a combined XANES and XRD study", *J. Magn. Magn. Mater.*, **323**(10), 1203-1206. https://doi.org/10.1016/j.jmmm.2010.11.006.

Goswami, P.P., Choudhury, H.A., Chakma, S. and Moholkar, V.S. (2013a), "Sonochemical synthesis and characterization of manganese ferrite nanoparticles", *Ind. Eng. Chem. Res.*, **52**(50), 17848-17855. https://doi.org/10.1021/ie401919x.

Goswami, P. P., Choudhury, H. A., Chakma, S. and Moholkar, V. S. (2013b), "Sonochemical synthesis of cobalt ferrite nanoparticles", *Int. J. Chem. Eng.*, **2013**, 1-6. https://doi.org/10.1155/2013/934234.

Grandjean, F. and Long, G.J. (2021), "Best practices and protocols in Mössbauer spectroscopy", *Chem. Mater.*, **33**(11), 3878-3904. https://doi.org/10.1021/acs.chemmater.1c00326.

Gul, S., Yousuf, M.A., Anwara, A., Warsi, M.F., Agboola, P.O., Shakir, I., Shahid, M. (2020), "Al-substituted zinc spinel ferrite nanoparticles: Preparation and evaluationof structural, electrical, magnetic and photocatalytic properties" *Ceram. Int.*, **46**(9), 14195-14205. https://doi.org/10.1016/j.ceramint.2020.02.228.

Hammad, A., Hemdan, B. and Elnahrawy, A. (2020), "Facile synthesis and potential application of $Ni_{0.6}Zn_{0.4}Fe_2O_4$ and $Ni_{0.6}Zn_{0.2}Ce_{0.2}Fe_2O_4$ magnetic nanocubes as a new strategy in sewage treatment", *J. Environ. Manag.*, **270**, 110816. https://doi.org/10.1016/j.jenvman.2020.110816.

Hashhash, A., Bobrikov, I., Yehia, M., Kaiser, M. and Uyanga, E. (2020), "Neutron diffraction and Mössbauer spectroscopy studies for Ce doped $CoFe_2O_4$ nanoparticles", *J. Magn. Magn. Mater.*, **503**, 166624. https://doi.org/10.1016/j.jmmm.2020.166624.

Hayek, S.S. (2019), "Synthesis and characterization of CeGdZn-ferrite nanoparticles as magnetic hyperthermia application agents", *Adv. Mater. Sci. Eng.*, 4868506. https://doi.org/10.1155/2019/4868506.

Hazra, S. and Ghosh, N. (2014), "Preparation of nanoferrites and their applications", *Journal of nanoscience and nanotechnology*, **14**, 1983-2000. https://doi.org/10.1166/jnn.2014.8745.

Henderson, C.M.B., Charnock, J.M. and Plant, D.A. (2007), "Cation occupancies in Mg, Co, Ni, Zn, Al ferrite spinels: A multi-element EXAFS study", *J. Phys. Condens. Matter*, **19**(7), 076214. https://doi.org/10.1088/0953-8984/19/7/076214

Islam, K., Haque, M., Kumar, A., Hoq, A., Hyder, F. and Hoque, S. M. (2020), "Manganese ferrite nanoparticles ($MnFe_2O_4$): Size dependence for hyperthermia and negative/positive contrast enhancement in MRI", *Nanomater.*, **10**(11), 2297. https://doi.org/10.3390/nano10112297.

Ito, A., Shinkai, M., Honda, H. and Kobayashi, T. (2005), "Medical application of functionalized magnetic nanoparticles", *J. Biosci. Bioeng.*, **100**(1), 1-11. https://doi.org/10.1263/jbb.100.1

Jesudoss, S.K., Vijaya, J.J., Kennedy, L.J., Rajan, P.I., Al-Lohedan, H.A., Ramalingam, R.J., Kaviyarasu, K. and Bououdina, M. (2016), "Studies on the efficient dual performance of $Mn_{1-x}Ni_xFe_2O_4$ spinel nanoparticles in photodegradation and antibacterial activity", *J. Photochem. Photobiol. B*, **165**, 121-132. https://doi.org/10.1016/j.jphotobiol.2016.10.004.

Johnson, M., Gaffney, C., White, V., Bechelli, J., Balaraman, R. and Trad, T. (2020), "Non-hydrolytic synthesis of caprylate capped cobalt ferrite nanoparticles and their application against Erwinia carotovora and Stenotrophomonas maltophilia", *J. Mater. Chem. B*, **8**(47), 10845-10853. https://doi.org/10.1039/D0TB02283G.

Joshi, G.P., Saxena, N.S., Mangal, R., Mishra, A. and Sharma, T.P. (2003), "Band gap determination of Ni-Zn ferrites", *Bull. Mater. Sci.*, **26**(4), 387-389. https://doi.org/10.1007/BF02711181.

Kadyrzhanov, K.K., Egizbek, K., Kozlovskiy, A.L. and Zdorovets, M.V. (2019), "Synthesis and properties of ferrite-based nanoparticles", *Nanomaterials*, **9**(8), 1079. https://doi.org/10.3390/nano9081079.

Kefeni, K.K., Msagati, T.A.M. and Mamba, B.B. (2017), "Ferrite nanoparticles: Synthesis, characterisation and applications in electronic device", *Mater. Sci. Eng. B*, **215**, 37-55. https://doi.org/10.1016/j.mseb.2016.11.002.

Khalili, P. and Farahmandjou, M. (2020), "Nanofabrication of zinc ferrite ($ZnFe_2O_4$) composites for biomedical application", *Challenges Nano Micro Scale Sci. Technol.*, **8**(2), 89-98. https://doi.org/10.22111/tpnms.2020.35902.1199.

Kharisov, B.I., Dias, H.V.R. and Kharissova, O.V. (2019), "Mini-review: Ferrite nanoparticles in the catalysis", *Arab. J. Chem.*, **12**(7), 1234-1246. https://doi.org/10.1016/j.arabjc.2014.10.049.

Kim, W. and Saito, F. (2001), "Mechanochemical synthesis of zinc ferrite from zinc oxide and α-Fe_2O_3", *Powder Technol.*, **114**(1-3), 12-16. https://doi.org/10.1016/S0032-5910(00)00256-4.

Klencsár, Z., Kuzmann, E. and Vértes, A. (1996), "User-friendly software for Mössbauer spectrum analysis", *J. Radioanal. Nuclear Chem.*, **210**(1), 105-118. https://doi.org/10.1007/BF02055410.

Kozakova, Z., Kuřitka, I., Bazant, P., Machovsky, M., Pastorek, M., Babayan, V. and Ltd, T. (2012), "Simple and effective preparation of cobalt ferrite nanoparticles by microwave-assisted solvothermal method", *Proceedings of the 4th International Conference*, Brno, Czech republic.

Kumar, H., Singh, J., Srivastava, R., Patel, K. and Chae, K.H. (2017), "Synthesis and characterization of $Dy_xCoFe_{2-x}O_4$ nanoparticles", *Superlatt. Microstruct.*, **109**, 296-306. https://doi.org/10.1016/j.spmi.2017.05.001.

Kumar, H., Srivastava, R.C., Singh, J.P., Negi, P., Agrawal, H.M., Das, D. and Chae, K.H. (2016), "Structural and magnetic study of dysprosium substituted cobalt ferrite nanoparticles", *J. Magn. Magn. Mater.*, **401**, 16-21. https://doi.org/10.1016/j.jmmm.2015.09.077.

Kumar, M., Dosanjh, H.S., Sonika, Singh, J., Monir, K. and Singh, H. (2020), "Review on magnetic nanoferrites and their composites as alternatives in waste water treatment: synthesis, modifications and applications", *Environ. Sci. Water Res. Technol.*, **6**(3), 491-514. https://doi.org/10.1039/C9EW00858F.

Kurtinaitienė, M., Mazeika, K., Ramanavičius, S., Pakštas, V. and Jagminas, A. (2016), "Effect of additives on the hydrothermal synthesis of manganese ferrite nanoparticles", *Adv. Nano Res.*, **4**(1), 1-14. https://doi.org/10.12989/anr.2016.4.1.001.

Lai, J., Shafi, K.V.P.M., Ulman, A., Loos, K., Yang, N.L., Cui, M.H., Vogt, T., Estournès, C. and Locke, D.C. (2004), "Mixed iron−manganese oxide nanoparticles", *J. Phys. Chem. B*, **108**(39), 14876-14883. https://doi.org/10.1021/jp049913w.

Lazarević, Z.Ž., Jovalekić, Č., Ivanovski, V.N., Rečnik, A., Milutinović, A., Cekić, B. and Romčević, N.Ž. (2014), "Characterization of partially inverse spinel $ZnFe_2O_4$ with high saturation magnetization synthesized via soft mechano-chemically assisted route", *J. Phys. Chem. Solids*, **75**(7), 869-877. https://doi.org/10.1016/j.jpcs.2014.03.004.

Lee, I.J., Yu, C.J., Yun, Y.D., Lee, C.S., Seo, I.D., Kim, H.Y., Lee, W.W. and Chae, K.H. (2010), "Note: Construction of x-ray scattering and x-ray absorption fine structure beamline at the Pohang Light Source", *Rev. Sci. Instrum.*, **81**(2), 026103. https://doi.org/10.1063/1.3298581.

Lee, P.Y., Chang, S.P. and Chang, S.J. (2013), "Synthesis and optical properties of ZnO thin films prepared by SILAR method with ethylene glycol", *Adv. Nano Res.*, **1**(2), 93-103. http://doi.org/10.12989/anr.2013.1.2.093.

Li, H., Wu, H.Z. and Xiao, G.X. (2010), "Effects of synthetic conditions on particle size and magnetic properties of $NiFe_2O_4$", *Powder Technol.*, **198**(1), 157-166. https://doi.org/10.1016/j.powtec.2009.11.005.

Li, W., Lee, S.S., Wu, J., Hinton, C.H. and Fortner, J.D. (2016), "Shape and size controlled synthesis of uniform iron oxide nanocrystals through new non-hydrolytic routes", *Nanotechnology*, **27**(32), 324002. https://doi.org/10.1088/0957-4484/27/32/324002.

Li, Z., Gao, K., Han, G., Wang, R., Li, H., Zhao, X. and Guo, P. (2015), "Solvothermal synthesis of $MnFe_2O_4$ colloidal nanocrystal assemblies and their magnetic and electrocatalytic properties", *New J. Chem.*, **39**(1), 361-368. https://doi.org/10.1039/C4NJ01466A.

Ma, J., Chen, B., Chen, B. and Zhang, S. (2017), "Preparation of superparamagnetic $ZnFe_2O_4$ submicrospheres via a solvothermal method", *Adv. Nano Res.*, **5**(2), 171-178. https://doi.org/10.12989/anr.2017.5.2.171.

Manova, E., Kunev, B., Paneva, D., Mitov, I., Petrov, L., Estournès, C., D'Orléan, C., Rehspringer, J.L. and Kurmoo, M. (2004), "Mechano-synthesis, characterization, and magnetic properties of nanoparticles of cobalt ferrite, $CoFe_2O_4$", *Chem. Mater.*, **16**(26), 5689-5696. https://doi.org/10.1021/cm049189u.

Marinca, T., Chicinas, I. and Isnard, O. (2012), "Synthesis, structural and magnetic characterization of nanocrystalline $CuFe_2O_4$ as obtained by a combined method reactive milling, heat treatment and ball milling", *Ceram. Int.*, **38**(3), 1951-1957. https://doi.org/10.1016/j.ceramint.2011.10.026.

Marinca, T.F., Chicinaş, I., Isnard, O., Pop, V. and Popa, F. (2011), "Synthesis, structural and magnetic characterization of nanocrystalline nickel ferrite—$NiFe_2O_4$ obtained by reactive milling", *J. Alloys Compd.*, **509**(30), 7931-7936. https://doi.org/10.1016/j.jallcom.2011.05.040.

Matsnev, M.E. and Rusakov, V.S. (2012), "SpectrRelax: an application for Mössbauer spectra modeling and fitting", *AIP Conference Proceedings*, **1489**(1), 178-185. https://doi.org/10.1063/1.4759488.

Morales-Flores, N., Galeazzi, R., Rosendo, E., Diaz, T. and Pal, U. (2013), "Morphology control and optical properties of ZnO nanostructures grown by ultrasonic synthesis", *Adv. Nano Res.*, **1**(1), 59-70. http://doi.org/10.12989/anr.2013.1.1.059.

Mozaffari, M. and Masoudi, H. (2014), "Zinc ferrite nanoparticles: New preparation method and magnetic properties", *J. Superconduct. Novel Magn.*, **27**(11), 2563-2567. https://doi.org/10.1007/s10948-014-2625-x.

Mukhtar, M.W., Irfan, M., Ahmad, I., Ali, I., Akhtar, M.N., Khan, M.A., Abbas, G., Rana, M.U., Ali, A. and Ahmad M. (2015), "Synthesis and properties of Pr-substituted MgZn ferrites for core materials and high frequency applications", *J. Magn. Magn. Mater.*, **381**, 173-178. https://doi.org/10.1016/j.jmmm.2014.12.072.

Munir, S., Rasheed, A., Zulfiqar, S., Aadil, M., Agboola, P.O., Shakir, I., Warsi, M.F. (2020)," Synthesis, characterization and photocatalytic parameters investigation of a new $CuFe_2O_4/Bi_2O_3$ nanocomposite", *Ceram. Int.*, **46** (18A), 29182-29190. https://doi.org/10.1016/j.ceramint.2020.08.091.

Muret, P. (1974), "Optical absorption in polycrystalline thin films of magnetite at room temperature", *Solid State Commun.*, **14**(11), 1119-1122. https://doi.org/10.1016/0038-1098(74)90286-5.

Murphy, D.M. (2008), *EPR (Electron Paramagnetic Resonance) Spectroscopy of Polycrystalline Oxide Systems*, In *Metal Oxide Catalysis*, Wiley-VCH: Strauss GmbH, Morlenbach, **1**, 1-50.

Nachbaur, V., Tauvel, G., Verdier, T., Jean, M., Juraszek, J. and Houvet, D. (2009), "Mecanosynthesis of partially inverted zinc ferrite", *J. Alloys Compd.*, **473**(1), 303-307. https://doi.org/10.1016/j.jallcom.2008.05.066.

Nakashima, S., Fujita, K., Tanaka, K., Hirao, K., Yamamoto, T. and Tanaka I. (2007), "First-principles XANES simulations of spinel zinc ferrite with a disordered cation distribution", *Phys. Rev. B*, **75**(17), 174443. https://doi.org/10.1103/PhysRevB.75.174443.

Nassar, M.Y. and Khatab, M. (2016), "Cobalt ferrite nanoparticles via a template-free hydrothermal route as an efficient nano-adsorbent for potential textile dye removal", *RSC Adv.*, **6**(83), 79688-79705. https://doi.org/10.1039/C6RA12852A.

Ni, D., Lin, Z., Xiaoling, P., Xinqing, W. and Hongliang, G. (2015), "Preparation and characterization of nickel-zinc ferrites

by a solvothermal method", *Rare Metal Mater. Eng.*, **44**(9), 2126-2131. https://doi.org/10.1016/S1875-5372(16)30010-8.

Oliver, S.A., Harris, V.G., Hamdeh, H.H. and Ho, J.C. (2000), "Large zinc cation occupancy of octahedral sites in mechanically activated zinc ferrite powders", *Appl. Phys. Lett.*, **76**(19), 2761-2763. https://doi.org/10.1063/1.126467.

Olsson, R.T., Alvarez, G.S., Hedenqvist, M.S., Gedde, U.W., Lindberg, F. and Savage, S. J. (2005), "Controlled synthesis of near-stoichiometric cobalt ferrite nanoparticles", *Chem. Mater.*, **17**(20), 5109-5118. https://doi.org/10.1021/cm0501665.

Pal, U., Madrid, U.S., and Jesús, F.D. (2014), "Controlling size and magnetic properties of Fe_3O_4 clusters in solvothermal process", *Adv. Nano Res.*, **2**(4), 187-198. http://doi.org/10.12989/anr.2014.2.4.187.

Palla, B.J., Shah, D., Casillas, P.E.G. and Matutes-Aquino, J.A. (1999), "Preparation of nanoparticles of barium ferrite from precipitation in microemulsions", *J. Nanoparticle Res.*, **1**, 215-221. https://doi.org/10.1023/A:1010004616528.

Pang, Y.L., Lim, S., Ong, H.C. and Chong, W.T. (2016), "Research progress on iron oxide-based magnetic materials: Synthesis techniques and photocatalytic applications", *Ceram. Int.*, **42**(1), 9-34. https://doi.org/10.1016/j.ceramint.2015.08.144.

Parc, Y.W., Kim, C., Huang, J.Y. and Ko, I.S. (2009), "The coherency of synchrotron radiation at Pohang Accelerator Laboratory", *J. Synchrotron Radiat.*, **16**(5), 642-646. https://doi.org/10.1107/S0909049509024649.

Parmar, H., Upadhyay, R.V., Rayaprol, S. and Siruguri, V. (2015), "Size induced inverse spins canting in CO–Zn system: Neutron diffraction and magnetic studies", *J. Magn. Magn. Mater.*, **377**, 133-136. https://doi.org/10.1016/j.jmmm.2014.10.071.

Patange, S.M., Shirsath, S.E., Jadhav, S.S., Lohar, K.S., Mane, D.R. and Jadhav, K.M. (2010), "Rietveld refinement and switching properties of Cr^{3+} substituted $NiFe_2O_4$ ferrites", *Mater. Lett.*, **64**(6), 722-724. https://doi.org/10.1016/j.matlet.2009.12.049.

Pemartin, K., Solans, C., Quintana, J.A. and Sanchez-Dominguez, M. (2014), "Synthesis of Mn–Zn ferrite nanoparticles by the oil-in-water microemulsion reaction method", *Colloids Surf. A Phys.*, **451**, 161-171. https://doi.org/10.1016/j.colsurfa.2014.03.036.

Peng, Y., Xia, C., Cui, M., Yao, Z. and Yi, X. (2021), "Effect of reaction condition on microstructure and properties of $(NiCuZn)Fe_2O_4$ nanoparticles synthesized via co-precipitation with ultrasonic irradiation", *Ultrasonics Sonochem.*, **71**, 105369. https://doi.org/10.1016/j.ultsonch.2020.105369.

Pereira, C., Pereira, A.M., Fernandes, C., Rocha, M., Mendes, R., Fernández-García, M.P., Guedes, A., Tavares, P.B., Grenèche, J.M., Araújo, J.P. and Freire, C. (2012), "Superparamagnetic MFe_2O_4 (M = Fe, Co, Mn) nanoparticles: Tuning the particle size and magnetic properties through a novel one-step coprecipitation route", *Chem. Mater.*, **24**(8), 1496-1504. https://doi.org/10.1021/cm300301c.

Pouponneau, P., Leroux, J.C. and Martel, S. (2009), "Magnetic nanoparticles encapsulated into biodegradable microparticles steered with an upgraded magnetic resonance imaging system for tumor chemoembolization", *Biomater.*, **30**(31), 6327-6332. https://doi.org/10.1016/j.biomaterials.2009.08.005.

Rahman, A. Aadil, M., Akhtar, M., Warsi, M.F., Jamil, A., Shakir, I., Shahid, M. (2020), "Magnetically recyclable $Ni_{1-x}Cd_xCe_yFe_{2-y}O_4$-rGO nanocomposite photocatalyst for visible light driven photocatalysis", *Ceram. Int.*, **46**(9), 13517-13526. https://doi.org/10.1016/j.ceramint.2020.02.136.

Rai, R.S. and Bajpai, V. (2021), "Recent advances in ZnO nanostructures and their future perspective", *Adv. Nano Res.*, **11**(1), 37-54. http://doi.org/10.12989/anr.2021.11.1.037.

Ramachandran, T. and Vishista, K. (2014), "N-N-methylene bis acrylamide: A novel fuel for combustion synthesis of zinc ferrite nanoparticles and studied by x-ray photoelectron spectroscopy", *Int. J. ChemTech Res.*, **6**(5), 2834-2842.

Rashdan, S.A. and Hazeem, L.J. (2020), "Synthesis of spinel ferrites nanoparticles and investigating their effect on the growth of microalgae Picochlorum sp", *Arab J. Basic Appl. Sci.*, **27**(1), 134-141. https://doi.org/10.1080/25765299.2020.1733174.

Ravel, B. and Newville, M. (2005), "ATHENA, ARTEMIS, HEPHAESTUS: Data analysis for X-ray absorption spectroscopy using IFEFFIT", *J. Synchrotr. Radiat.*, **12**(4), 537-541. https://doi.org/10.1107/S0909049505012719.

Reddy, D.H.K. and Yun, Y.S. (2016), "Spinel ferrite magnetic adsorbents: alternative future materials for water purification?", *Coordinat. Chem. Rev.*, **315**, 90-111. https://doi.org/10.1016/j.ccr.2016.01.012.

Sagadevan, S., Chowdhury, Z.Z. and Rafique, R.F. (2018), "Preparation and characterization of nickel ferrite nanoparticles via co-precipitation method", *Mater. Res.*, **21**(2), 1-5. https://doi.org/10.1590/1980-5373-MR-2016-0533.

Sathiyamurthy, K., Rajeevgandhi, C., Bharanidharan, S., Sugumar, P. and Bose, S. (2020), "Electrochemical and magnetic properties of zinc ferrite nanoparticles through chemical co-precipitation method", *Chem. Data Collect.*, **28**, 100477. https://doi.org/10.1016/j.cdc.2020.100477.

Scano, A., Cabras, V., Pilloni, M. and Ennas, G. (2019), "Microemulsions: The renaissance of ferrite nanoparticle synthesis", *J. Nanosci. Nanotechnol.*, **19**(8), 4824-4838. https://doi.org/10.1166/jnn.2019.16876.

Schmitt-Rink, S., Miller, D.A.B. and Chemla, D.S. (1987), "Theory of the linear and nonlinear optical properties of semiconductor microcrystallites", *Phys. Rev. B*, **35**(15), 8113-8125. https://doi.org/10.1103/PhysRevB.35.8113.

Sharma, A., Singh, J., Won, S.O., Chae, K.H., Sharma, S.K. and Kumar, S. (2018), *Introduction to X-Ray Absorption Spectroscopy and Its Applications in Material Science*, In *Handbook of Materials Characterization*, Springer International Publishing.

Sharma, R., Bansal, S. and Singhal, S. (2015), "Tailoring the photo-Fenton activity of spinel ferrites (MFe_2O_4) by incorporating different cations (M = Cu, Zn, Ni and Co) in the structure", *RSC Advances*, **5**(8), 6006-6018. https://doi.org/10.1039/C4RA13692F.

Shirsath, S., Wang, D., Jadhav, S., Mane, M. and Li, S. (2017), *Ferrites Obtained by Sol–Gel Method*, In *Handbook of Sol-Gel Science and Technology*, Springer, Cham.

Singh, J., Dixit, G., Srivastava, R., Kumar, H. and Agrawal, H. (2013a), "Magnetic resonance in superparamagnetic zinc ferrite", *Bull. Mater. Sci.*, **36**(4), 751-754. https://doi.org/10.1007/s12034-013-0528-2.

Singh, J.P., Dixit, G., Pandey, K., Kumar, H., Srivastava, R.C., Agrawal, H.M. and Asokan, K. (2014), "Spin dynamics investigation in nanosized zinc ferrite irradiated with 200 MeV Ag^{15+} ions", *Mater. Lett.*, **122**, 277-280. https://doi.org/10.1016/j.matlet.2014.02.019.

Singh, J.P., Dixit, G., Srivastava, R.C., Agrawal, H.M. and Kumar, R. (2013b), "Raman and Fourier-transform infrared spectroscopic study of nanosized zinc ferrite irradiated with 200 MeV Ag^{15+} beam", *J. Alloys Compd.*, **551**, 370-375. https://doi.org/10.1016/j.jallcom.2012.10.006.

Singh, J.P., Dixit, G., Srivastava, R.C., Agrawal, H.M., Reddy, V.R. and Gupta, A. (2012), "Observation of bulk like magnetic ordering below the blocking temperature in nanosized zinc ferrite", *J. Magn. Magn. Mater.*, **324**(16), 2553-2559. https://doi.org/10.1016/j.jmmm.2012.03.045.

Singh, J.P., Dixit, G., Srivastava, R.C., Negi, P., Agrawal, H.M. and Kumar, R. (2013c), "HRTEM and FTIR investigation of

nanosized zinc ferrite irradiated with 100 MeV oxygen ions", *Spectrochimica Acta Part A*, **107**, 326-333. https://doi.org/10.1016/j.saa.2012.12.095.

Singh, J.P., Kim, S.H., Won, S.O., Lim, W.C., Lee, I.J. and Chae, K.H. (2016), "Covalency, hybridization and valence state effects in nano- and micro-sized $ZnFe_2O_4$", *CrystEngComm*, **18**(15), 2701-2711. https://doi.org/10.1039/C5CE02461G.

Singh, J.P., Lee, B.H., Lim, W.C., Shim, C.H., Lee, J. and Chae, K. H. (2018), "Microstructure, local electronic structure and optical behaviour of zinc ferrite thin films on glass substrate", *Royal Soc. Open Sci.*, **5**(10), 181330. https://doi.org/10.1098/rsos.181330.

Singh, J.P., Srivastava, R.C. and Agrawal, H.M. (2010), "Optical behaviour of zinc ferrite nanoparticles", *AIP Conference Proceedings*, **1276**(1), 137-143. https://doi.org/10.1063/1.3504278.

Singh, J.P., Srivastava, R.C., Agrawal, H.M. and Chand, P. (2009), "Relaxation phenomena in nanostructured zinc ferrite", *Int. J. Nanosci.*, **08**(6), 523-531. https://doi.org/10.1142/s0219581x09006456.

Singh, J.P., Srivastava, R.C., Agrawal, H.M., Chand, P. and Kumar, R. (2011a), "Observation of size dependent attributes on the magnetic resonance of irradiated zinc ferrite nanoparticles", *Curr. Appl. Phys.*, **11**(3), 532-537. https://doi.org/10.1016/j.cap.2010.09.009.

Singh, J.P., Srivastava, R.C., Agrawal, H.M. and Kumar, R. (2011b), "100 MeV O7+ ion irradiation in nanosized zinc ferrite", *Radiat. Effects Defects Solids*, **166**(8-9), 564-570. https://doi.org/10.1080/10420150.2011.553233.

Singh, J.P., Srivastava, R.C., Agrawal, H.M. and Kumar, R. (2011c), "Micro-Raman investigation of nanosized zinc ferrite: Effect of crystallite size and fluence of irradiation", *J. Raman Spectrosc.*, **42**(7), 1510-1517. https://doi.org/10.1002/jrs.2902

Singh, J.P., Srivastava, R.C., Agrawal, H.M., Kushwaha, R.P.S., Chand, P. and Kumar, R. (2008), "EPR study of nanostructured zinc ferrite", *Int. J. Nanosci.*, **07**(1), 21-27. https://doi.org/10.1142/s0219581x08005146.

Singh, R.S., Kuřitka, I., Vilcakova, J., Jamatia, T., Machovsky, M., Skoda, D., Urbánek, P., Masař, M., Urbánek, M., Kalina, L. and Havlica, J. (2020), "Impact of sonochemical synthesis condition on the structural and physical properties of $MnFe_2O_4$ spinel ferrite nanoparticles", *Ultrasonics Sonochem.*, **61**, 104839. https://doi.org/10.1016/j.ultsonch.2019.104839.

Sivakumar, M., Towata, A., Yasui, K., Tuziuti, T. and Iida, Y. (2006), "A new ultrasonic cavitation approach for the synthesis of zinc ferrite nanocrystals", *Curr. Appl. Phys.*, **6**(3), 591-593. https://doi.org/10.1016/j.cap.2005.11.068.

Sivakumar, M., Towata, A., Yasui, K., Tuziuti, T., Kozuka, T., Iida, Y., Maiorov, M.M., Blums, E., Bhattacharya, D., Sivakumar, N. and Ashok, M. (2012), "Ultrasonic cavitation induced water in vegetable oil emulsion droplets – a simple and easy technique to synthesize manganese zinc ferrite nanocrystals with improved magnetization", *Ultrasonics Sonochem.*, **19**(3), 652-658. https://doi.org/10.1016/j.ultsonch.2011.10.015.

Sivakumar, P., Ramesh, R., Ramanand, A., Ponnusamy, S. and Muthamizhchelvan, C. (2011), "Preparation of sheet like polycrystalline $NiFe_2O_4$ nanostructure with PVA matrices and their properties", *Mater. Lett.*, **65**(9), 1438-1440. https://doi.org/10.1016/j.matlet.2011.02.026.

Song, Q. and Zhang, Z.J. (2012), "Controlled synthesis and magnetic properties of bimagnetic spinel ferrite $CoFe_2O_4$ and $MnFe_2O_4$ nanocrystals with core–shell architecture", *J. Am. Chem. Soc.*, **134**(24), 10182-10190. https://doi.org/10.1021/ja302856z.

Springer, V., Pecini, E. and Avena, M. (2016), "Magnetic nickel ferrite nanoparticles for removal of dipyrone from aqueous solutions", *J. Environ. Chem. Eng.*, **4**(4), 3882-3890. https://doi.org/10.1016/j.jece.2016.08.026.

Stewart, S.J., Figueroa, S.J.A., López, J.M.R., Marchetti, S.G., Bengoa, J.F., Prado, R.J. and Requejo, F.G. (2007), "Cationic exchange in nanosized $ZnFe_2O_4$ spinel revealed by experimental and simulated near-edge absorption structure", *Phys. Rev. B*, **75**(7), 073408. https://doi.org/10.1103/PhysRevB.75.073408.

Su, M., He, C. and Shih, K. (2016), "Facile synthesis of morphology and size-controlled α-Fe_2O_3 and Fe_3O_4 nano-and microstructures by hydrothermal/solvothermal process: The roles of reaction medium and urea dose", *Ceram. Int.*, **42**(13), 14793-14804. https://doi.org/10.1016/j.ceramint.2016.06.111

Syahmazgi, M., Falamaki, C. and Lotfi, A. (2014), "A novel method for the synthesis of nano-magnetite particles", *Adv. Nano Res.*, **2**(2), 89-98. http://doi.org/10.12989/anr.2014.2.2.089.

Tadjarodi, A., Imani, M. and Salehi, M. (2015), "$ZnFe_2O_4$ nanoparticles and a clay encapsulated $ZnFe_2O_4$ nanocomposite: synthesis strategy, structural characteristics and the adsorption of dye pollutants in water", *RSC Adv.*, **5**(69), 56145-56156. https://doi.org/10.1039/C5RA02163D.

Tanaka, K., Nakashima, S., Fujita, K. and Hirao, K. (2006), "Large Faraday effect in a short wavelength range for disordered zinc ferrite thin films", *J. Appl. Phys.*, **99**(10), 106103. https://doi.org/10.1063/1.2199727.

Tang, Y., Wang, X., Zhang, Q., Li, Y. and Wang, H. (2012), "Solvothermal synthesis of $Co_{1-x}Ni_xFe_2O_4$ nanoparticles and its application in ammonia vapors detection", *Prog. Natural Sci. Mater. Int.*, **22**(1), 53-58. https://doi.org/10.1016/j.pnsc.2011.12.009.

Tauc, J. (1974), *Optical Properties of Amorphous Semiconductors*, In *Amorphous and Liquid Semiconductors*, Springer Boston, MA, U.S.A.

Tauc, J. and Menth, A. (1972), "States in the gap", *J. Non Cryst. Solids*, **8-10**, 569-585. https://doi.org/10.1016/0022-3093(72)90194-9.

Thota, S., Kashyap, S.C., Sharma, S.K. and Reddy, V.R. (2016), "Micro Raman, Mossbauer and magnetic studies of manganese substituted zinc ferrite nanoparticles: Role of Mn", *J. Phys. Chem. Solids*, **91**, 136-144. https://doi.org/10.1016/j.jpcs.2015.12.013.

Todaka, Y., Nakamura, M., Hattori, S., Tsuchiya, K. and Umemoto, M. (2003), "Synthesis of ferrite nanoparticles by mechanochemical processing using a ball mill", *Mater. Transact.*, **44**(2), 277-284. https://doi.org/10.2320/matertrans.44.277.

Torres, I.Z., Dominguez, A.S., Bueno, J.J.P. and Lopez, M.L.M. (2021), "Analyzing corrosion rates of TiO_2 nanotubes/titanium separation passive layer under surface and crystallization changes", *Adv. Nano Res.*, **10**(3), 211-219. https://doi.org/10.12989/anr.2021.10.3.211.

Upadhyay, C. and Verma, H.C. (2004), "Anomalous change in electron density at nuclear sites in nanosize zinc ferrite", *Appl. Phys. Lett.*, **85**(11), 2074-2076. https://doi.org/10.1063/1.1786368.

Upadhyay, C., Verma, H.C., Sathe, V. and Pimpale, A.V. (2007), "Effect of size and synthesis route on the magnetic properties of chemically prepared nanosize $ZnFe_2O_4$", *J. Magn. Magn. Mater.*, **312**(2), 271-279. https://doi.org/10.1016/j.jmmm.2006.10.448.

Urbach, F. (1953), "The long-wavelength edge of photographic sensitivity and of the electronic absorption of solids", *Phys. Rev.*, **92**(5), 1324-1324. https://doi.org/10.1103/PhysRev.92.1324.

Ushakov, M.V., Senthilkumar, B., Selvan, R.K., Felner, I. and Oshtrakh, M.I. (2017), "Mössbauer spectroscopy of $NiFe_2O_4$ nanoparticles: The effect of Ni^{2+} in the Fe^{3+} local micro-

environment in both tetrahedral and octahedral sites", *Mater. Chem. Phys.*, **202**, 159-168. https://doi.org/10.1016/j.matchemphys.2017.09.011.

Venkatesh, M., Kumar, G.S., Viji, S., Karthi, S. and Girija, E.K. (2016), "Microwave assisted combustion synthesis and characterization of nickel ferrite nanoplatelets", *Modern Electr. Mater.*, **2**(3), 74-78. https://doi.org/10.1016/j.moem.2016.10.003.

Wang, Z., Lazor, P., Saxena, S.K. and Artioli, G. (2002), "High-pressure Raman spectroscopic study of spinel ($ZnCr_2O_4$)", *J. Solid State Chem.*, **165**(1), 165-170. https://doi.org/10.1006/jssc.2002.9527.

Yan, Z., Gao, J., Li, Y., Zhang, M. and Guo, M. (2015), "Hydrothermal synthesis and structure evolution of metal-doped magnesium ferrite from saprolite laterite", *RSC Adv.*, **5**(112), 92778-92787. https://doi.org/10.1039/C5RA17145H.

Yáñez-Vilar, S., Sánchez-Andújar, M., Gómez-Aguirre C., Mira, J., Señarís-Rodríguez, M.A. and Castro-García, S. (2009), "A simple solvothermal synthesis of MFe_2O_4 (M=Mn, Co and Ni) nanoparticles", *J. Solid State Chem.*, **182**(10), 2685-2690. http://doi.org/10.1016/j.jssc.2009.07.028.

Yao, T., Qi, Y., Mei, Y., Yang, Y., Aleisa, R., Tong, X. and Wu, J. (2019), "One-step preparation of reduced graphene oxide aerogel loaded with mesoporous copper ferrite nanocubes: a highly efficient catalyst in microwave-assisted Fenton reaction", *J. Hazard. Mater.*, **378**, 120712. https://doi.org/10.1016/j.jhazmat.2019.05.105.

Yin, Y., Liu, W., Huo, N. and Yang, S. (2017), "Synthesis of vesicle-like $MgFe_2O_4$/graphene 3D network anode material with enhanced lithium storage performance", *ACS Sust. Chem. Eng.*, **5**(1), 563-570. https://doi.org/10.1021/acssuschemeng.6b01949

Yu, S.H., Wang, Q.L., Chen, Y., Wang, Y. and Wang, J.H. (2020), "Microwave-assisted synthesis of spinel ferrite nanospherolites", *Mater. Lett.*, **278**, 128431. https://doi.org/10.1016/j.matlet.2020.128431.

Zeng, Y., Zhu, X., Xie, J. and Chen, L. (2021), "Ionic liquid coated magnetic core/shell $CoFe_2O_4@SiO_2$ nanoparticles for the separation/analysis of trace gold in water sample", *Adv. Nano Res.*, **10**(3), 295-312. https://doi.org/10.12989/anr.2021.10.3.295

Zhang, L. and Wu, Y. (2013), "Sol-gel synthesized magnetic $MnFe_2O_4$ spinel ferrite nanoparticles as novel catalyst for oxidative degradation of methyl orange", *J. Nanomater.*, 1-6. https://doi.org/10.1155/2013/640940.

Zhi-hao, Y., Wei, Y., Jun-hui, J. and Li-de, Z. (2008), "Optical absorption red shift of capped $ZnFe_2O_4$ nanoparticle", *Chinese Phys. Lett.*, **15**(7), 535. https://doi.org/10.1088/0256-307X/15/7/024.

Zhu, H., Gu, X., Zuo, D., Wang, Z., Wang, N. and Yao K. (2008), "Microemulsion-based synthesis of porous zinc ferrite nanorods and its application in a room-temperature ethanol sensor", *Nanotechnology*, **19**(40), 405503. https://doi.org/10.1088/0957-4484/19/40/405503.

JL